DISCLAIMER NOTICE

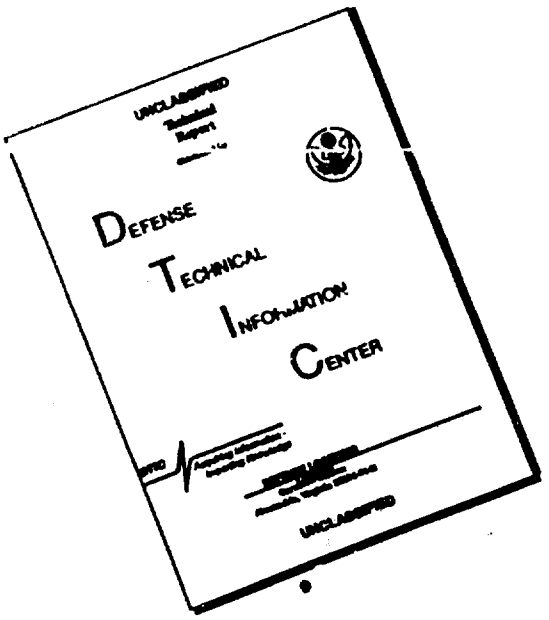

THIS DOCUMENT IS BEST QUALITY AVAILABLE. THE COPY FURNISHED TO DTIC CONTAINED A SIGNIFICANT NUMBER OF PAGES WHICH DO NOT REPRODUCE LEGIBLY.

AD-A268 281

ATION PAGE

Form Approved
OBM No. 0704 0188

1. Agency Use Only (Leave blank).	2. Report Date.	3. Report Type and Dates Covered.
	July 1993	Final - Journal Article

4. Title and Subtitle.
Sensitivity of Satellite Multichannel Sea Surface Temperature Retrievals to the Air-Sea Temperature Difference

5. Funding Numbers.
Program Element No. 0603704N
Project No. 010
Task No. 100
Accession No. DN394457
Work Unit No. 93212F

6. Author(s).
Douglas A. May and Ronald J. Holyer

7. Performing Organization Name(s) and Address(es).
Naval Research Laboratory
Remote Sensing Applications Branch
Stennis Space Center, MS 39529-5004

8. Performing Organization Report Number.
JA 321:067:92

9. Sponsoring/Monitoring Agency Name(s) and Address(es).
Space and Naval Warfare Systems Command
Washington, DC

10. Sponsoring/Monitoring Agency Report Number.
JA 321:067:92

11. Supplementary Notes.
Published in Journal of Geophysical Research.

12a. Distribution/Availability Statement.
Approved for public release; distribution is unlimited.

12b. Distribution Code.

13. Abstract *(Maximum 200 words).*

The advanced very high resolution radiometer multichannel sea surface temperature (MCSST) retrieval technique provides global algorithm accuracy statistics generally showing a bias of less than 0.15°C and an rms error of less than 0.7°C when compared to colocated drifting buoy in situ data in the absence of aerosols. This remaining error is not always random but is shown to be correlated to the air-sea temperature difference. The MCSST technique is modeled and then compared to in situ data to show this dependency. Atmospheric radiative transfer calculations are used to provide a simulation of satellite retrieval sensitivity to air-sea temperature differences. Buoy sea surface temperature (SST) and air temperature observations are then presented as experimental verification of the simulation results. Retrieval errors depend both on the mean air-sea temperature difference conditions present in the data set used to empirically derive the algorithm and on the changes in air-sea temperature difference conditions relative to the derivation data set mean conditions.

93 8 18 068

93-18818

14. Subject Terms.
Remote sensing, thermodynamic ocean models, satellite sea surface temperature

15. Number of Pages.
11

16. Price Code.

17. Security Classification of Report.	18. Security Classification of This Page.	19. Security Classification of Abstract.	20. Limitation of Abstract.
Unclassified	Unclassified	Unclassified	SAR

JOURNAL OF GEOPHYSICAL RESEARCH, VOL. 98, NO. C7, PAGES 12,567–12,577, JULY 15, 1993

Sensitivity of Satellite Multichannel Sea Surface Temperature Retrievals to the Air-Sea Temperature Difference

DOUGLAS A. MAY AND RONALD J. HOLYER

Naval Research Laboratory, Remote Sensing Applications Branch, Stennis Space Center, Mississippi

The advanced very high resolution radiometer multichannel sea surface temperature (MCSST) retrieval technique provides global algorithm accuracy statistics generally showing a bias of less than 0.1°C and an rms error of less than 0.7°C when compared to colocated drifting buoy in situ data in the absence of aerosols. This remaining error is not always random but is shown to be correlated to the air-sea temperature difference. The MCSST technique is modeled and then compared to in situ data to show this dependency. Atmospheric radiative transfer calculations are used to provide a simulation of satellite retrieval sensitivity to air-sea temperature differences. Buoy sea surface temperature (SST) and air temperature observations are then presented as experimental verification of the simulation results. Retrieval errors depend both on the mean air-sea temperature difference conditions present in the data set used to empirically derive the algorithm and on the changes in air-sea temperature difference conditions relative to the derivation data set mean conditions. Retrieval error is found to respond linearly with air-sea temperature difference changes. MCSST retrieval errors of 1.0°C can occur for air-sea temperature difference changes of 7°–10°C from mean conditions when the dual-window (channels 3 and 4) or triple-window (channels 3, 4, and 5) algorithms are used. The split-window (channels 4 and 5) MCSST algorithm is shown to be less sensitive to air-sea temperature differences. Cross-product SST (CPSST) and nonlinear SST (NLSST) algorithms are also examined. These algorithms generate results similar to the MCSST algorithm for the dual- and triple-window equations. However, the CPSST and NLSST split-window algorithms demonstrate greater sensitivity to air-sea temperature difference changes than do the MCSST split-window algorithm. Retrieval errors of 1°C can occur for air-sea temperature difference changes of 10°–12°C from mean conditions. Users of satellite SST retrievals in regions that experience large fluctuations in air-sea temperature difference should be aware of this possible error source.

INTRODUCTION

The generation of absolute sea surface temperature (SST) from satellite infrared (IR) brightness temperature measurements has been studied often [*Anding and Kauth*, 1970; *Maul and Sidran*, 1972; *McMillin*, 1975; *Bernstein*, 1982; *Llewellyn-Jones et al.*, 1984; *McMillin and Crosby*, 1984; *Walton*, 1988; *Barton and Cechet*, 1989; *Barton et al.*, 1989]. Because the surface-emitted radiation is partially absorbed and reradiated by the atmosphere, an atmospheric correction must be made to the satellite-measured radiances before the (SST) can be determined. Typically, two or more IR measurements at differing wavelengths or viewing angles are used to determine this atmospheric correction [*McMillin and Crosby*, 1984].

Global multichannel sea surface temperature (MCSST) retrievals from satellites have been operationally produced from National Oceanic and Atmospheric Administration (NOAA) advanced very high resolution radiometer (AVHRR) data for several years at the National Environmental Satellite Data and Information Service (NESDIS) [e.g., *McClain*, 1989]. MCSSTs are retrieved globally each day on an orbit-by-orbit basis from global area coverage (GAC) data at a spatial resolution of 8 km (2 by 2 GAC arrays). Details about operational MCSST processing and cloud-screening algorithms are given by *McClain et al.* [1985].

Operational retrieval algorithms are empirically derived by regressing satellite retrievals to global drifting buoy SST data typically within 4 hours and 25 km [*Strong and McClain*, 1984]. This is routinely accomplished soon after satellite launch and rarely requires change until the next satellite launch. Through the use of cloud-screening algorithms and the increased quality and quantity of in situ data the accuracy of satellite data has improved to the point that present monthly global comparisons with drifting buoys generally show a bias of less than 0.1°C and an rms error of less than 0.7°C [*McClain*, 1989].

The use of the MCSST technique when large air-sea temperature differences exist can lead to reduced accuracy [*McMillin and Crosby*, 1984]. Air and sea surface temperature difference is often less than 2°C [*Isemer and Hasse*, 1985]; however, coastal locations can experience greater extremes. It is important to investigate the magnitude of global retrieval algorithm errors under such anomalous atmospheric conditions. Accurate knowledge of the coastal water environment is valuable to both military and commercial activities. Since coastal locations experience frequent air-sea temperature extremes not often observed in the deep ocean, identifying satellite retrieval errors under such conditions will enable us to develop improved retrieval techniques.

Studies using simulated retrieval algorithms have predicted satellite SST errors for regionally optimized algorithms when used under anomalous atmospheric conditions [e.g., *Minnett*, 1986; *Minnett*, 1990]. These errors were predicted to range from a few tenths of a degree to more than 1°C, depending on the algorithm employed. However, such predictions have not been verified with in situ data.

This paper investigates the sensitivity of multichannel SST retrieval techniques to air-sea temperature difference, hereinafter referred to as ASTD. A simple model is presented that predicts a dependence of retrieval errors on the ASTD.

Paper number 93JC00913.

The LOWTRAN 7 [*Kneizys et al.*, 1988] atmospheric radiative transfer model is then used to provide a simulated error prediction of the multichannel technique for significant ASTD. This predicted error is then confirmed utilizing coincident satellite SST retrievals, buoy SST, and buoy air temperature observations. In addition to the MCSST algorithm the more recent cross-product SST (CPSST) and nonlinear SST (NLSST) algorithms are also evaluated. The implications of these results and the identification of conditions under which satellite SST data are likely to be less accurate are then discussed.

THEORY

If one assumes that the atmosphere is a horizontally and vertically homogeneous absorbing but nonscattering medium and that the emissivity of the sea surface is at unity (implying that surface reflectivity is zero), the following simple radiative transfer equation results:

$$E_{\text{sat}} = \int_{\lambda_1}^{\lambda_2} \{\tau(\lambda)B(\lambda, T_s) + [1 - \tau(\lambda)]B(\lambda, T_a)\}\, d\lambda \quad (1)$$

where E_{sat} is the energy received at the satellite, $B(\lambda, T)$ is Planck's function for energy at wavelength λ emitted by a blackbody at temperature T, $\tau(\lambda)$ is the transmittance of the atmosphere at wavelength λ, T_s is the temperature of the sea surface, T_a is the mean temperature of the atmosphere, and λ_1 and λ_2 define the sensor spectral band pass.

Equation (1) describes radiative transfer in this simple model in terms of radiant energy. The radiative transfer equation expressed in terms of equivalent blackbody temperatures results in

$$T_{\text{sat}} = \tau T_s + (1 - \tau)T_a \quad (2)$$

where τ is the "effective" value of $\tau(\lambda)$ in the spectral band between λ_1 and λ_2. The temperature observed by the satellite sensor, T_{sat}, is equal to T_s only in the hypothetical case where $\tau = 1$.

Equation (2) cannot be solved directly for T_s, because it contains two unknowns, T_s and τ. However, two simultaneous equations can be obtained by sensing the ocean in two different spectral bands, hence the multichannel technique. A complete discussion of the multichannel solution theory can be found in *McMillin* [1975]. This relationship, expressed in terms of channel brightness temperature and atmospheric transmittance, results in

$$T_s = \left[\frac{1 - \tau_2}{\tau_1 - \tau_2}\right]T_1 - \left[\frac{1 - \tau_1}{\tau_1 - \tau_2}\right]T_2 \quad (3)$$

where T_1 and T_2 represent the IR channel brightness temperatures, respectively, and τ_1 and τ_2 represent the atmospheric transmittance for each channel bandwidth, respectively.

Figure 1 shows an atmospheric transmittance curve applicable to the LOWTRAN 7 U.S. Standard Atmosphere model. The spectral bands for AVHRR channels 3, 4, and 5 are also denoted in Figure 1. Note that a typical transmittance value for channel 3 is approximately 0.9, while a typical transmittance value for channel 4 is about 0.7. If these values are inserted in (3) as τ_1 and τ_2, the following MCSST algorithm is obtained:

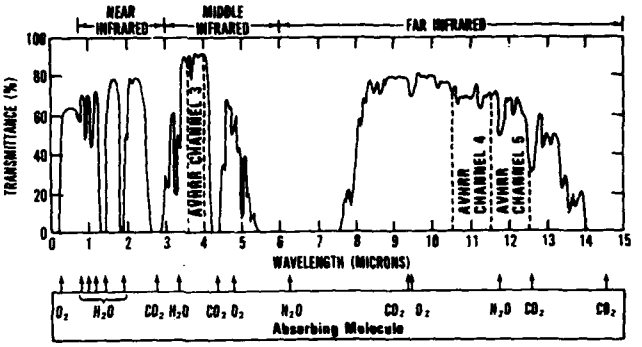

Fig. 1. The percent of transmittance of radiant energy as a function of wavelength for a wide spectral range for the U.S. Standard Atmosphere model, including the three AVHRR infrared channels [*LaViolette*, 1988].

$$T(3, 4) = 1.5T_3 - 0.5T_4 \quad (4)$$

where $T(3, 4)$ represents the SST obtained using AVHRR channels 3 and 4 and T_3 and T_4 represent channel 3 and channel 4 brightness temperatures, respectively.

A comparable empirical MCSST algorithm that NOAA derived from drifting buoy data and used operationally for NOAA 11 is

$$MC(3, 4) = 1.5866T_3 - 0.5905T_4 + 2.027[\sec(\theta) - 1] + 2.96 \quad (5)$$

where θ is the satellite zenith angle. The term containing the satellite zenith angle compensates for increased path length for off-nadir viewing. This correction for zenith angle allows for comparison of satellite observations from several AVHRR swath angles with the model results which, for simplicity, were calculated for vertical viewing only. The close correspondence between channel coefficients of the theoretical algorithm (4) and the empirical algorithm (5) indicates that the simple model actually does a fair job of depicting radiative transfer in the ocean-atmosphere system.

We now proceed to model errors in MCSST data. For the case of AVHRR IR channels 3 and 4, we can calculate the temperatures observed by the satellite using the radiative transfer equation (2). These simulated satellite observations can then be atmospherically corrected to give $T(3, 4)$ by using the theoretical MCSST algorithm (4). The resulting MCSST error E in $T(3, 4)$ can then be calculated:

$$E = T(3, 4) - T_s \quad (6)$$

or, after appropriate substitution and algebraic manipulation,

$$E = (1.5\tau_3 - 0.5\tau_4 - 1)(T_s - T_a) \quad (7)$$

Equation (7) demonstrates an error in MCSST that is a linear function of the difference between the sea surface and atmospheric temperatures. T_a is the temperature of the atmosphere which has been modeled as vertically uniform. In truth, atmospheric temperature varies with altitude. Thus (7) is difficult to compare with actual observations, as the variable T_a represents the mean effective atmospheric temperature.

For each atmosphere, LOWTRAN provides atmospheric temperatures for 32 levels. These temperatures can be

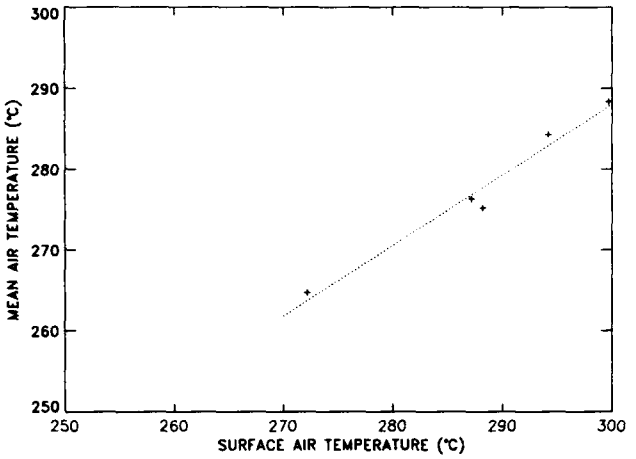

Fig. 2. Mean model atmospheric air temperature versus model surface air temperature for five LOWTRAN 7 atmospheric models. Dotted line represents linear regression relationship obtained in (8).

averaged over the altitudes representative of water vapor attenuation effects at IR wavelengths to obtain T_a, the mean effective atmospheric temperature for the spectral bands used. LOWTRAN contains six atmospheric models of which five are representative of general atmospheric conditions over the ocean surface where SST retrievals are typically obtained (70°N to 70°S). These models are the U.S. Standard, tropical, mid-latitude summer, mid-latitude winter, and Subarctic summer atmospheres.

Atmospheric model temperatures were averaged over levels ranging from the surface to 7 km. This altitude was selected because (1) water vapor is the major atmospheric attenuating medium at the wavelengths of interest and (2) the majority of atmospheric water vapor typically exists in the lowest 7 km, with more than half in the lowest 3 km [*U.S. Air Force*, 1965].

In Figure 2 the mean atmospheric temperature is plotted versus the model surface air temperature, which is assumed to be representative of the standard 10-m height. Although a limited number of atmospheric models are used, if one assumes that these models are generally representative of atmospheric conditions over the global ocean, the results demonstrate a basic linear relationship between model surface air temperature and mean model atmospheric temperature. This relationship can be expressed by

$$T_a = 0.874T_a(0) + 25.86 \tag{8}$$

where $T_a(0)$ represents the model surface air temperature. The regressed correlation coefficient between T_a and $T_a(0)$ is excellent ($R = 0.98$). The regression F statistic test assured that the model adequately accounts for a significant amount of variation in the response and that it explains mean atmospheric temperature at a 95% confidence level.

The value of T_a from (8) can now be substituted into (7) to provide MCSST errors in terms of the sea surface temperature and surface air temperature.

$$E = (1.5\tau_3 - 0.5\tau_4 - 1)[T_s - 0.874T_a(0) - 25.86] \tag{9}$$

Simulation Experiment

We employed the LOWTRAN 7 code to compute satellite-sensed apparent surface temperatures for various sea surface temperatures and atmospheric profiles for the three AVHRR IR channels. The NOAA 11 IR channel transfer functions were used to model the channel responses and generate the brightness temperatures for each simulated channel. These simulated brightness temperatures were then used to generate MCSST, CPSST, and NLSST retrievals under the five atmospheric model conditions mentioned previously.

To simulate the effects of ASTD, the model sea surface temperature was allowed to range 5°C above and below each atmospheric model surface air temperature at increments of 1°C. The error between simulated satellite SST algorithm retrievals and the sea surface temperature was then calculated at each step, providing the simulated retrieval error sensitivity to ASTD.

Satellite SST retrievals were obtained for the three IR channel combinations used operationally: dual-window (channels 3 and 4), split-window (channels 4 and 5), and triple-window (channels 3, 4, and 5). The simulation retrieval algorithms were generated from multiple linear regressions of the simulated IR channel brightness temperatures to model sea surface temperatures. For simplicity the retrieval algorithms were first derived using cases in which the sea surface temperatures equaled the model surface air temperatures (ASTD equal to zero). Algorithms were later derived at ±5°C ASTD to compare results. These results will be discussed later. The model MCSST algorithm simulation equations for zero ASTD are

$$T(3, 4) = 1.0283T_4 + 1.3116(T_3 - T_4) - 6.89 \tag{10}$$

$$T(3, 4, 5) = 1.0204T_4 + 0.9464(T_3 - T_5) - 4.73 \tag{11}$$

$$T(4, 5) = 1.0042T_4 + 3.2014(T_4 - T_5) - 0.36 \tag{12}$$

The operational NOAA 11 equation corresponding to $T(3, 4)$ was previously given in (5). The following are the operational triple- and split-window algorithms for NOAA 11.

$$MC(3, 4, 5) = 1.0095T_4 + 1.041(T_3 - T_5) + 1.76[\sec(\theta) - 1] - 2.04 \tag{13}$$

$$MC(4, 5) = 1.0561T_4 + 2.5415(T_4 - T_5) + 0.888(T_4 - T_5)[\sec(\theta) - 1] - 16.9795 \tag{14}$$

Differences between simulated and operational equations may be attributed to at least two factors: (1) the different methods employed to obtain the simulated versus operational equations and (2) the dependence of algorithm coefficients on ASTD. The operational NOAA 11 algorithms are generated empirically using several hundred global drifting buoy SSTs matched to satellite retrievals obtained under actual atmospheric conditions. In comparison, the model-simulated algorithms were generated from a limited number of atmospheric model temperatures that may or may not constitute an adequate sample of global conditions. Since water vapor continuum absorption coefficients in the thermal IR band are not precisely known, the model-simulated algorithm coefficients strongly depend on the transmission code used. The results obtained by this study, however, will show that ASTD error characteristics for model-simulated algorithms and operational algorithms are very similar.

The other likely factor producing coefficient differences

will be mentioned here and then expanded upon at the end of this section. It will be demonstrated that algorithms derived for a specific mean ASTD will differ from algorithms derived at other ASTD conditions and will be less accurate than the other algorithms at those conditions. Thus the mean ASTD present in the data set used to derive the SST algorithm will greatly influence the resultant equation coefficients and the equation's accuracy at other ASTD conditions.

Equations (10), (11), and (12) were derived assuming zero ASTD conditions. In reality the assumption that global mean ASTD is zero may not be true. This fact can be easily demonstrated by utilizing the in situ SST and air temperature data available from the global buoy data employed in this study. This data set reveals global buoy SST to be an average 1.04°C warmer than surface air temperature. Thus the operational equations derived from global buoy data would account for whatever mean ASTD exists in the data set used to derive the equations, leading to a difference between simulated and operational algorithm coefficients.

CPSST and NLSST algorithms were also evaluated. As described by *Walton* [1988], the CPSST algorithm assumes a nonlinear atmospheric correction based upon IR brightness temperature magnitude and interchannel temperature difference. The NLSST [*Walton et al.*, 1990] modifies this nonlinear technique to be a function of the underlying surface temperature. These techniques differ from MCSST, which assumes a linear atmospheric correction based solely upon interchannel temperature differences. The simulated and operational NOAA 11 CPSST and NLSST algorithms are listed in the appendix. The T_f term in the NLSST equations represents the underlying surface temperature obtained from an analysis field, climatology, or MCSST retrieval. This study used the latter value for T_f, applying the appropriate MCSST algorithm (5, 13, or 14).

Figure 3 depicts the simulated MCSST retrieval error for the three MCSST retrieval algorithms in each of the model atmospheres. The dual-, split-, and triple-window algorithm errors are denoted by solid, dotted, and dashed lines, respectively. Each algorithm was derived assuming zero ASTD, and it is interesting to note that with few exceptions, each is most accurate under such conditions. Also, note that the simulated dual-window and triple-window algorithms consistently overestimate SST when the air temperature is much warmer than the underlying sea surface and underestimate SST when conditions are reversed. The split-window algorithm shows much less consistent sensitivity to ASTD.

The slopes for these error lines are presented in Table 1. These values were obtained via a linear least squares fit of the error at each 1°C increment. Slope t statistics were calculated for each fit at the 95% confidence level to test the hypothesis that the true slope may actually equal zero. Those slope values with t statistics not found to be statistically significant are enclosed in parentheses. The hypothesis that the slope is actually zero cannot be rejected for such cases. Note that only two model split-window slopes can be identified statistically as nonzero. The overall trend for the other two algorithms is a statistically significant slope that varies by only a small amount between atmospheric models.

Both the dual-window and triple-window algorithms indicate significant MCSST retrieval error in all model atmospheres as the difference between the sea surface temperature and the air temperature increases. This finding predicts the MCSST retrieval to be colder than the true sea surface temperature when the air temperature is significantly less than the sea surface temperature. Similarly, the MCSST retrieval is predicted to be warmer than the true sea surface temperature when the air temperature is substantially greater than the sea surface temperature. Taking an average of the simulated slope values, the dual-window algorithm error is approximately 1°C for every 7°C change in the ASTD. For the triple-window algorithm the simulation predicts a 1°C error for every 10°C change in the ASTD.

The split-window algorithm only shows significant slope for tropical and mid-latitude winter atmospheres with no statistically significant slope for the other atmospheric models. These predictions indicate that the dual-window and triple-window MCSST algorithms should be more sensitive to the ASTD than is the split-window algorithm. This finding is generally expected, since the MCSST algorithm assumes that the atmospheric absorption process is similar at the two wavelengths used for the atmospheric correction. Such assumptions are obviously more valid for channels 4 and 5 [*Prabhakara et al.*, 1974], which are centered within 1 μm of each other.

Tables 2 and 3 display the predicted slopes for CPSST and NLSST errors, respectively. Although the dual- and triple-window error slopes are comparable to the respective MCSST algorithm errors, both the CPSST and NLSST split-window algorithms demonstrate greater sensitivity to the ASTD than does the MCSST split-window algorithm. These split-window algorithms may be in error 1°C for every 10°–12°C change in ASTD. These results differ from the MCSST split-window results which do not show consistent sensitivity. This difference may be due to the increased dependence of the CPSST algorithm on the brightness temperature magnitude and to the NLSST algorithm dependence on the underlying surface temperature magnitude. Not surprisingly, this dependence makes the algorithms more sensitive to ASTD changes.

As stated previously, simulation equations were also derived under model-simulated conditions in which the ASTD was nonzero, specifically, ±5°C. The resulting algorithms generated error slopes nearly identical to the respective algorithms in Tables 1–3. However, the error magnitudes, or bias, of each algorithm were displaced approximately 0.5°C on either side of the slope lines generated from the zero ASTD algorithms.

An example of this is shown in Figure 4 for the U.S. Standard Atmosphere model dual-window algorithm. This figure clearly shows that an algorithm derived under one mean ocean-atmosphere relationship will not be as accurate under other ocean-atmosphere conditions. Each, however, is most accurate when ASTD equals the mean conditions used to derive it. Other simulated retrieval algorithms and model atmospheres generated similar results regarding slope and algorithm error bias. This difference demonstrates the importance of the mean air-sea temperature contrast used to derive each simulated algorithm.

This result agrees with the findings of *Eyre* [1987] which demonstrated that retrieval errors are minimized for physical ocean-atmosphere situations that equal the mean ocean-atmosphere state used to derive the algorithm. An algorithm derived under zero ASTD will perform best for such conditions. Likewise, an algorithm derived from ASTD of 5°C will be less accurate than the first algorithm at zero ASTD but more accurate at 5°C difference.

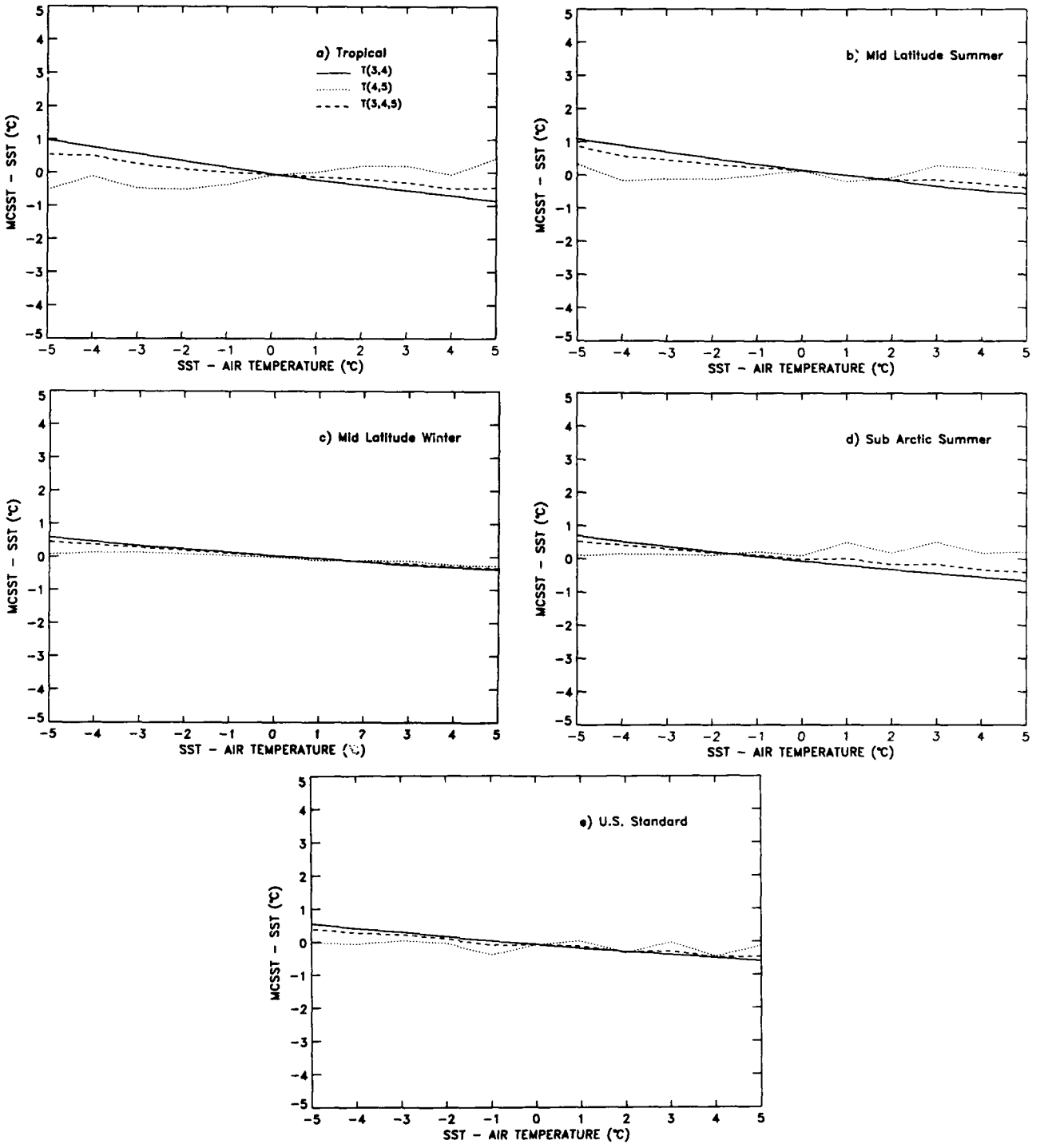

Fig. 3. Simulated MCSST retrieval error as a function of SST-air temperature difference by model atmosphere for each of three nighttime algorithms. Dual window (channels 3 and 4) is denoted by a solid line. Split window (channels 4 and 5) is denoted by a dotted line. Triple window (channels 3, 4, and 5) is denoted by a dashed line. (*a*) Tropical, (*b*) mid-latitude summer, (*c*) mid-latitude winter, (*d*) Subarctic summer, and (*e*) U.S. Standard.

Although algorithms can be generated to reduce the error bias at specific mean ocean-atmosphere states, the error of each algorithm is still sensitive to changes in the actual ASTD. This is clearly evident in Figure 4. Each algorithm is most accurate at the mean ASTD used to derive it. However, each algorithm error also follows approximately the same slope with respect to ASTD changes. Thus ASTD changes will have similar effects on regionally as well as globally derived algorithm accuracies. Such effects will be negligible only if ASTD varies less than a few degrees from mean conditions.

GROUND TRUTH COMPARISONS

Operational satellite retrievals are matched in near–real time to colocated buoy measurements as part of the NESDIS

TABLE 1. Predicted MCSST Error Slopes

Atmospheric Model	$T(3, 4)$ Slope	$T(4, 5)$ Slope	$T(3, 4, 5)$ Slope
Tropical	−0.184	0.079	−0.103
Midlatitude summer	−0.168	(0.010)	−0.114
Midlatitude winter	−0.097	−0.041	−0.081
Subarctic summer	−0.136	(0.020)	−0.090
U.S. Standard	−0.140	(0.009)	−0.095
Average	−0.145	0.015	−0.097

TABLE 3. Predicted NLSST Error Slopes

Atmospheric Model	$T(3, 4)$ Slope	$T(4, 5)$ Slope	$T(3, 4, 5)$ Slope
Tropical	−0.142	−0.045	−0.070
Midlatitude summer	−0.166	−0.129	−0.130
Midlatitude winter	−0.107	−0.128	−0.090
Subarctic summer	−0.148	−0.125	−0.120
U.S. Standard	−0.132	−0.112	−0.107
Average	−0.139	−0.108	−0.103

operational retrieval generation process. These matches are retained in a matchup data base that can be used for subsequent off-line analysis. Colocated satellite and buoy SST matchups were obtained from this data base for the months of February through May 1991. Matchups with moored and drifting buoys were collected globally to provide a diverse sample of matchups in all seasons.

For an ideal comparison the in situ and spaceborne sensors should measure the same quantity, which would require the use of a near-surface infrared radiometer. Since buoys typically measure SST at a depth of 1 m, it is argued that these "bulk SST" measurements can be decoupled from the true surface temperature by near-surface temperature gradients, the so-called "skin effect" [*Robinson et al.*, 1984; *Hepplewhite*, 1989].

Given that infrared radiometer in situ measurements from research ships are quite scarce and very regionalized [e.g., *Schluessel et al.*, 1987; *Coppin et al.*, 1991] and that atmospheric and oceanographic models and analyses traditionally assimilate bulk SST, it is very convenient to regress the satellite retrievals to this more readily available parameter. Use of a regionally derived in situ radiometer algorithm as a global algorithm can also be questioned because of the limited spatial and seasonal extent of the matchup comparisons used to generate the algorithm. Buoys provide a globally diverse set of observations accurate to 0.1°C that can be readily used to generate global algorithms and monthly global accuracy statistics.

In order to limit the time and distance variability that can occur between buoy and satellite data the matchups used in this study include only those buoy observations within 1 hour and 10 km of each satellite retrieval. *Minnett* [1991] demonstrates that such time and distance criteria provide representative matchups by eliminating possible temporal and spatial differences that might occur between satellite and in situ data because of diurnal SST changes or ocean frontal gradients.

Because some satellite retrievals are matched to more than one buoy observation, the data set was refined to include just the single closest buoy matchup in time and distance to each retrieval. The matchups were further restricted to nighttime-only satellite retrievals to avoid diurnal effects. The resulting data set includes 160 matchups obtained from most ocean regions of the world (Figure 5).

Using (5), AVHRR channels 3 and 4 brightness temperatures were used to calculate MC (3, 4) for each of the 160 satellite-buoy matchups. Figure 6 shows the NESDIS dual-window MCSST retrievals minus buoy SST versus the buoy SST minus air temperature. Note the negative slope of a satellite minus buoy values evident in Figure 6 as the buoy SST minus air temperature values increase. A simple least squares regression fit to the data results in a satellite minus buoy error slope of −0.143 with a standard error of 0.03 at the 95% confidence level.

To test whether the true value of the slope is equal to zero, the critical t statistic is calculated to be 1.645 for 158 degrees of freedom at the 95% confidence level. The regression model slope t statistic is found to be −3.507, which rejects the hypothesis that the true slope is equal to zero. The regression slope is therefore found to be statistically significant. The average slope of −0.145 predicted from the model atmospheres is within the standard error of the in situ data slope estimate. These encouraging results confirm the simulation experiment predictions of dual-window retrieval errors approaching 1°C for every 7°C change in the ASTD.

Figure 7 displays the NESDIS triple-window MCSST algorithm retrievals minus buoy SST versus the buoy SST minus air temperature. These results were obtained using

TABLE 2. Predicted CPSST Error Slopes

Atmospheric Model	$T(3, 4)$ Slope	$T(4, 5)$ Slope	$T(3, 4, 5)$ Slope
Tropical	−0.155	−0.053	−0.087
Midlatitude summer	−0.158	−0.090	−0.106
Midlatitude winter	−0.132	−0.044	−0.060
Subarctic summer	−0.145	−0.058	−0.082
U.S. Standard	−0.133	−0.056	−0.080
Average	−0.145	−0.060	−0.083

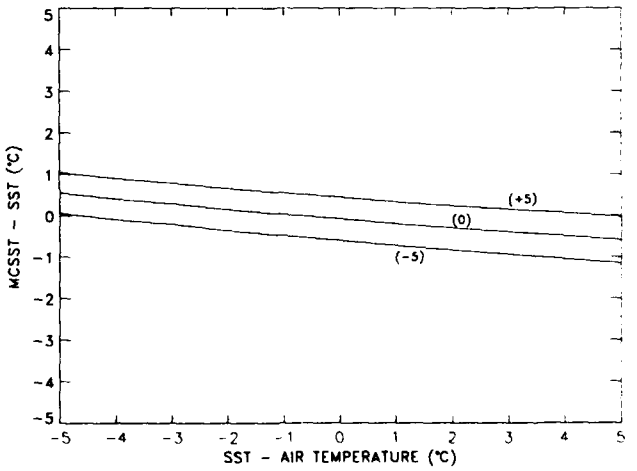

Fig. 4. Simulated dual-window MCSST retrieval error as a function of SST-air temperature difference for the U.S. Standard Atmosphere model. The three lines represent errors associated with model-simulated MCSST algorithms derived under three different air-sea temperature conditions: plus 5 (+5), zero (0), and minus 5 (−5).

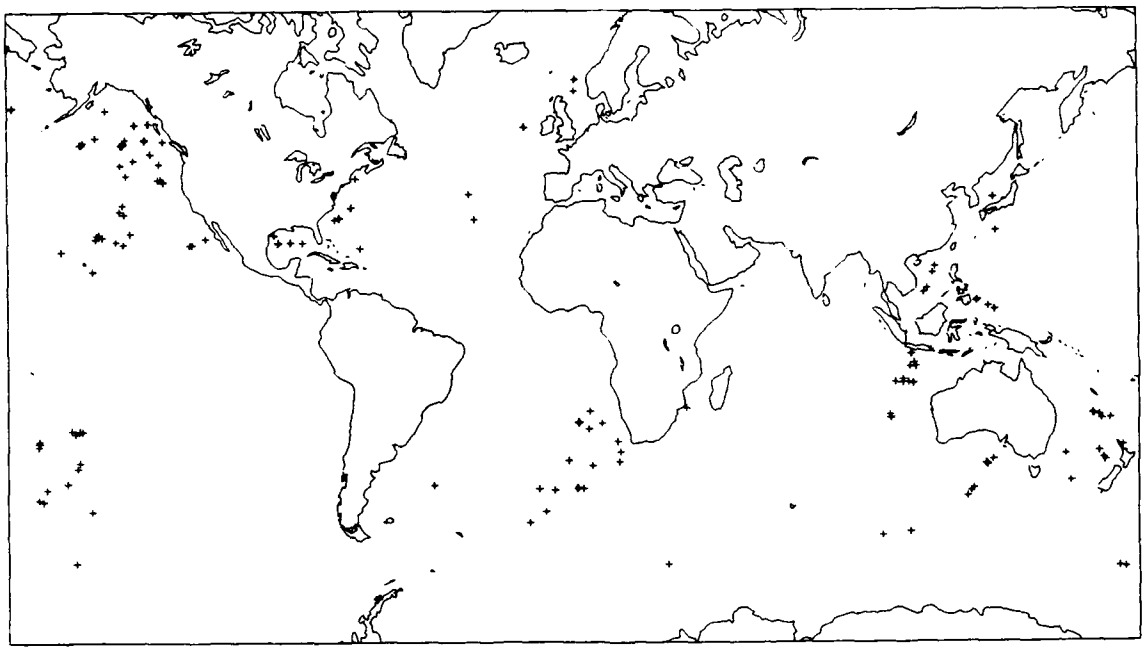

Fig. 5. Location of buoy in situ data used in data analysis. Each satellite-buoy matchup location is denoted by a plus.

(13). Like the dual-window algorithm, a negative slope is evident in the figure. A simple least squares regression fit to the data results in a satellite minus buoy error slope of −0.101 with a standard error of 0.03. The regression model slope t statistic is calculated to be −3.426, which is statistically significant at the 95% confidence level. This slope agrees quite well with the average slope of −0.097 predicted by the simulation experiment. These results predict satellite retrieval errors approaching 1°C for ASTD changes of 10°C.

Figure 8 shows the NESDIS split-window MCSST algorithm retrievals minus buoy SST versus the buoy ASTD. These results were obtained using (14). This figure indicates a more random distribution of matchups with ASTD than does the previous figures. A simple least squares regression fit predicts a slope of −0.043 with a standard error of 0.044. The slope t statistic is calculated as −0.969, which is not statistically significant at the 95% confidence level. Thus the hypothesis that the true slope value is zero cannot be rejected. This result is in general agreement with the simulation experiment, which indicated no significant slope with ASTD except for the tropical atmosphere.

Table 4 lists the error slopes for each algorithm type when compared to the buoy matchup data set. Similar to the MCSST algorithms, the average CPSST and NLSST versus buoy error slopes were found to be within the standard error of each slope predicted by the model atmospheres. These matchup results agree favorably with the simulated predictions, showing the dual-window and triple-window algorithms to be more sensitive to ASTD than is the split-window algorithm, especially for the MCSST technique.

Table 4 also shows that the nonlinear CPSST and NLSST split-window algorithms are more sensitive to ASTD than is the MCSST split-window algorithm. This difference was also demonstrated in the model predictions. Thus both model

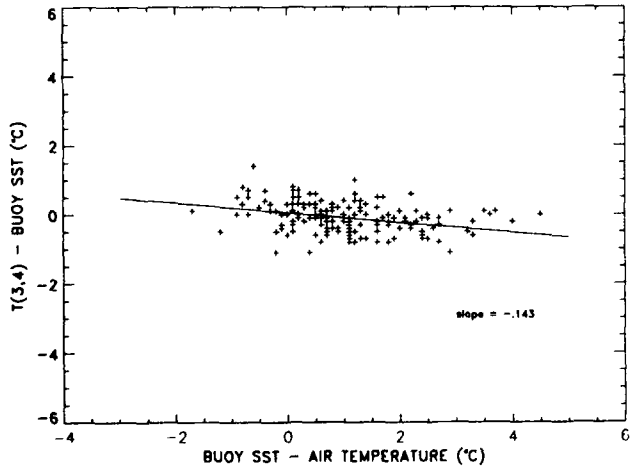

Fig. 6. MCSST dual-window retrieval minus buoy SST plotted versus the buoy SST minus buoy air temperature.

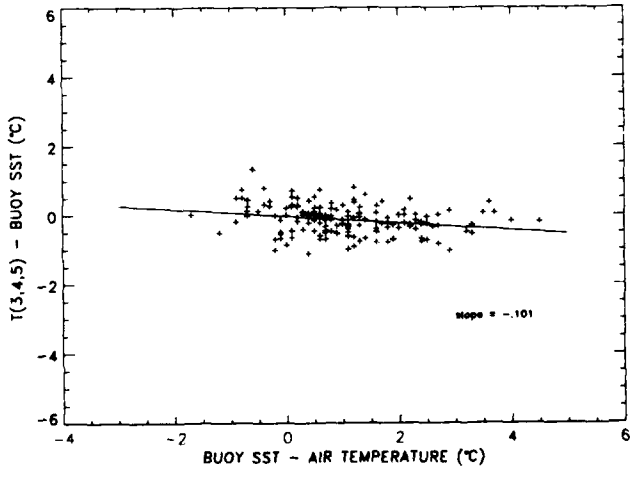

Fig. 7. MCSST triple-window retrieval minus buoy SST plotted versus the buoy SST minus buoy air temperature.

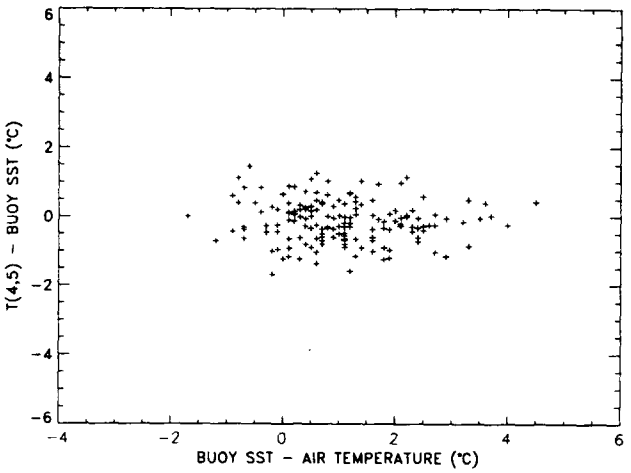

Fig. 8. MCSST split-window retrieval minus buoy SST plotted versus the buoy SST minus buoy air temperature.

predictions and ground truth comparisons indicate that use of satellite SST retrievals under extremely anomalous conditions of ASTD can generate significant retrieval errors.

Table 5 lists the mean bias and root mean square difference (rmsd) for each operational algorithm as compared to global buoy SSTs. The table displays global as well as regional statistics. The statistics have also been divided into atmospheric moisture classes, using the channel 4 minus 5 values as a measure of atmospheric moisture content and the buoy SST minus air temperature (BSST minus AT) to classify statistics by air-sea interface conditions.

In general, large positive BSST minus AT corresponds to large negative retrieval bias. Similarly, negative or very low positive BSST minus AT corresponds to positive or very low negative retrieval bias. This supports the model results obtained earlier, demonstrating that when air temperature is significantly greater (less) than SST, the satellite retrieval will overestimate (underestimate) SST

This result is not evident in all cases, particularly the split-window MCSST retrievals which are less sensitive to ASTD. The biases observed in the MCSST split-window algorithm regional cells are more a result of sensitivity to the 4 minus 5 values or atmospheric moisture content. Some of the largest negative biases in Table 5 are present in these cells. It appears that the split-window retrievals are too cold when the channel 4 minus 5 values are very small and too warm when conditions are reversed.

The nonlinear CPSST and NLSST algorithms improve on the MCSST split-window algorithm error quite nicely, reducing bias and rmsd in almost every region. These statistics demonstrate the improved retrieval accuracy that can be obtained using a nonlinear split-window algorithm. The exception to this is when the air temperature exceeds SST and when SST substantially exceeds air temperature. These results demonstrate the increased sensitivity of the CPSST and NLSST split-window algorithms to ASTD.

Comparison between the dual-, split-, and triple-window techniques shows that the triple-window algorithms demonstrate better overall rmsd statistics than the others. The triple-window algorithm bias statistic, however, is significantly sensitive to ASTD changes. The dual-window algorithms also demonstrate significant bias sensitivity as ASTD changes. This sensitivity is somewhat greater than the triple-window algorithm, as evidenced in the rows depicting ASTD conditions.

Overall, none of the 160 BSST minus AT matchups exceeded 5°C or were less than −2°C. This limited range of difference is related to the general world ocean situation in which the majority of ASTDs are less than ±2°C. The formation of cloud or fog as the temperature difference reaches one extreme or the other may also impair limits on these upper and lower thresholds. Thus, although such conditions could potentially cause significantly erroneous satellite SST retrievals, cloud formation would prevent the generation of satellite retrievals.

Derivation of regionally exclusive retrieval algorithms may not be an adequate solution to the ASTD sensitivity of retrievals. ASTD is a continually changing quantity, and one regional algorithm will not always serve a specific region's range of ASTD conditions unless ASTD never varies more than a few degrees. Use of air temperature information could possibly provide improved retrieval accuracy when large ASTD does exist. Air temperature information would need to have a fine enough time and spatial resolution that its use would not generate errors greater than those being corrected. Operational applications would be best served by air temperature information that is both temporally (within 1 hour) and spatially (within 10–20 km) accurate. However, given the present spatial resolution of global analyses and the relatively rapid changes that can occur in air temperature, operational use of such information is conjectured to be inadequate for present needs.

TABLE 4. Buoy Matchup Error Slopes

SST Algorithm	$T(3, 4)$ Slope	$T(4, 5)$ Slope	$T(3, 4, 5)$ Slope
MCSST	−0.143	(−0.043)	−0.101
CPSST	−0.136	−0.84	−0.105
NLSST	−0.143	−0.106	−0.129

Discussion and Conclusions

A simple model has been developed that predicts the dependence of MCSST satellite retrieval errors on the ASTD. A simulation experiment has been performed to test this dependence. Three satellite retrieval algorithms, the dual-window (channels 3 and 4), the split-window (channels 4 and 5), and the triple-window (channels 3, 4, and 5), plus the nonlinear CPSST and NLSST, were simulated and compared. Simulation results have also been compared to global buoy SST and air temperature data matched to satellite retrievals within specific time and distance constraints. It is evident from the comparisons that the model results simulate the effect of ASTD present in the satellite-buoy matchups and that the use of satellite SST retrievals under anomalous ASTD conditions can generate significant retrieval errors.

In general, when the actual ASTD is close to the mean ASTD conditions present in the algorithm derivation data set, the satellite retrieval algorithm will approximate ground truth SST measurements quite well. However, it is also revealed that global satellite retrievals can overestimate SST when the SST minus air temperature difference significantly

TABLE 5. Satellite/Buoy Matchup Statistics for the World and Various Global Regions

Region	Number of Matches	Mean SST-AT	Mean T4-T5	MC (34) (Bias) rmsd	MC (345) (Bias) rmsd	MC (45) (Bias) rmsd	CP (34) (Bias) rmsd	CP (345) (Bias) rmsd	CP (45) (Bias) rmsd	NL (34) (Bias) rmsd	NL (345) (Bias) rmsd	NL (45) (Bias) rmsd
World	160	1.04	1.27	(−0.10) 0.45	(−0.12) 0.44	(−0.01) 0.62	(−0.05) 0.45	(−0.03) 0.45	(−0.01) 0.53	(−0.11) 0.46	(−0.1[illegible] 0.44	(−0.07) 0.48
30N-70N	53	1.27	0.95	(−0.18) 0.45	(−0.32) 0.50	(−0.42) 0.67	(−0.24) 0.47	(−0.29) 0.50	(−0.32) 0.52	(−0.18) 0.46	(−0.22) 0.46	(−0.31) 0.48
30N-30S	58	1.17	1.62	(−0.14) 0.43	(−0.11) 0.39	(−0.12) 0.54	(0.01) 0.39	(0.04) 0.38	(0.04) 0.52	(−0.16) 0.46	(−0.10) 0.42	(0.01) 0.52
30S-70S	49	0.63	1.20	(0.05) 0.50	(0.08) 0.46	(0.29) 0.67	(0.07) 0.51	(0.16) 0.48	(0.26) 0.56	(0.02) 0.48	(0.04) 0	(0.12) 0.43
NE Pacific	51	1.32	0.98	(−0.10) 0.45	(−0.24) 0.50	(−0.33) 0.71	(−0.13) 0.48	(−0.20) 0.52	(−0.26) 0.59	(−0.11) 0.45	(−0.10) 0.46	(−0.26) 0.53
West Pacific	64	0.86	1.54	(−0.11) 0.41	(−0.05) 0.38	(0.19) 0.63	(−0.02) 0.40	(0.06) 0.39	(0.12) 0.54	(−0.13) 0.42	(−0.06) 0.39	(0.05) 0.48
North Atlantic	24	0.87	1.25	(−0.10) 0.42	(−0.11) 0.39	(0.08) 0.49	(−0.01) 0.41	(0.03) 0.40	(0.07) 0.41	(−0.12) 0.45	(−0.09) 0.42	(−0.01) 0.40
South Atlantic	21	1.09	1.17	(−0.04) 0.66	(−0.06) 0.57	(0.07) 0.58	(−0.01) 0.58	(0.03) 0.51	(0.08) 0.51	(−0.07) 0.67	(−0.06) 0.59	(−0.01) 0.47
0<T4 − T5<1	60	0.75	0.80	(−0.01) 0.49	(−0.23) 0.52	(−0.43) 0.67	(−0.05) 0.50	(−0.18) 0.52	(−0.25) 0.51	(0.01) 0.47	(−0.07) 0.46	(−0.19) 0.44
1<T4 − T5<2	82	1.23	1.37	(−0.14) 0.44	(−0.06) 0.42	(0.28) 0.60	(−0.06) 0.43	(0.06) 0.42	(0.16) 0.54	(−0.19) 0.45	(−0.13) 0.44	(0.0) 0.49
2<T4 − T5<3	18	1.12	2.36	(−0.16) 0.45	(−0.04) 0.30	(0.10) 0.59	(−0.03) 0.38	(0.05) 0.31	(−0.04) 0.57	(−0.16) 0.52	(−0.03) 0.42	(0.05) 0.57
−2<SST − AT<0	23	−0.55	0.99	(0.18) 0.57	(0.08) 0.57	(0.06) 0.76	(0.15) 0.56	(0.14) 0.59	(0.15) 0.63	(0.18) 0.57	(0.16) 0.55	(0.12) 0.49
0<SST − AT<2	104	0.87	1.30	(−0.09) 0.43	(−0.13) 0.43	(−0.03) 0.63	(−0.03) 0.42	(−0.03) 0.44	(−0.03) 0.53	(−0.11) 0.43	(−0.09) 0.41	(−0.01) 0.48
2<SST − AT<5	33	2.68	1.37	(−0.30) 0.48	(−0.22) 0.41	(0.02) 0.50	(−0.26) 0.48	(−0.15) 0.39	(−0.07) 0.47	(−0.33) 0.52	(−0.28) 0.47	(−0.20) 0.49

Statistics are also divided into atmospheric moisture classes, parameterized by the channel 4 minus channel 5 values; and also divided into ocean-atmosphere interface classes, parameterized by the buoy SST minus buoy air temperature values.

exceeds the mean difference present in the algorithm derivation data set. Likewise, retrievals can underestimate SST when conditions are reversed. Dual-window satellite retrievals may be in error 1°C for every 7°C change in ASTD from the mean conditions. Likewise, triple-window retrievals may be in error 1°C for every 10°C change in ASTD.

The split-window retrievals demonstrate less consistent sensitivity to ASTD except for the nonlinear CPSST and NLSST algorithms. The lack of sensitivity to ASTD in the MCSST method is most likely a result of the linear atmospheric correction technique and the proximity of channels 4 and 5 (10.5 and 11.5 μm). Since channel 3 is centered at 3.7 μm, the assumption that atmospheric absorption is similar in each IR channel is less valid for the dual- and triple-window algorithms than for the split-window algorithm. The nonlinear CPSST and NLSST split-window algorithms demonstrate greater dependence on the channel brightness temperature and underlying surface temperature magnitudes, resulting in greater sensitivity to ASTD changes. Nonlinear split-window retrieval algorithm errors of 1°C can occur for 10°–12°C changes in ASTD.

In conclusion, satellite-derived SSTs in ocean regions susceptible to extreme ASTD conditions may be suspect when using an algorithm derived under less extreme conditions. Such circumstances could generate significant satellite retrieval errors. Equations can be derived to attain better accuracy for extreme atmospheric situations; however, these equations would demonstrate significant error when air-sea temperature conditions become less extreme. Thus selection of regionally exclusive algorithms may not be an adequate solution, because ASTD is nonstatic, and one regional algorithm will not always serve that specific region's range of ASTD conditions unless the range is less than a few degrees.

Retrieval accuracy could theoretically improve by incorporating regionally accurate air temperature information into the algorithm. Operational use of currently available global analysis information is, however, probably inadequate owing to analysis spatial resolution and the relatively rapid air temperature changes that can occur between analysis products. Satellite SST retrieval users should thus be aware of both the mean atmosphere-ocean state used to derive the SST algorithm in use and the ASTD conditions to which it is applied. Results demonstrate that satellite retrieval errors of 0.1° to 0.14°C are possible for every degree that ASTD differs from the mean atmosphere-ocean state used to derive the algorithm.

APPENDIX: SIMULATED AND OPERATIONAL CPSST AND NLSST ALGORITHMS

Simulated

$$CP(3, 4) = 0.9951T_4 + \left(\frac{0.0736T_4 - 19.5579}{0.074T_4 - 0.0383T_3 - 9.0576}\right) \cdot (T_3 - T_4 + 1.0048) - 271.74$$

$$CP(3, 4, 5) = 0.9953T_4 + \left(\frac{0.0737T_4 - 19.5618}{0.0975T_5 - 0.038T_3 - 15.261}\right) \cdot (T_3 - T_5 + 1.303) - 271.82$$

$$CP(4, 5) = 0.9955T_5 + \left(\frac{0.0971T_5 - 26.04}{0.0975T_5 - 0.074T_4 - 6.26}\right) \cdot (T_4 - T_5 + 0.239) - 271.89$$

$$NL(3, 4) = 1.0311T_3 + 0.00925T_f(T_3 - T_4) - 280.84$$

$$NL(3, 4, 5) = 1.0238T_4 + 0.7351(T_3 - T_5) + 0.00682T_f(T_3 - T_5) - 278.87$$

$$NL(4, 5) = 1.0302T_4 + 0.8884T_f(T_4 - T_5) - 280.73$$

Operational

$$CP(3, 4) = 0.9853T_4 + \left(\frac{0.1708T_4 - 58.47}{0.17334T_4 - 0.0775T_3 - 33.74}\right) \cdot (T_3 - T_4 - 6.44) + 1.97[\sec(\theta) - 1] - 257.28$$

$$CP(3, 4, 5) = 0.9712T_4 + \left(\frac{0.1684T_4 - 34.32}{0.2052T_5 - 0.0775T_3 - 20.01}\right)(T_3 - T_5 + 14.86) + 1.87(\sec(\theta) - 1) - 276.59$$

$$CP(4, 5) = 0.9548T_5 + \left(\frac{0.1960T_5 - 48.61}{0.2052T_5 - 0.1733T_4 - 6.11}\right) \cdot (T_4 - T_5 + 1.46) + 0.98(T_4 - T_5) \cdot [\sec(\theta) - 1] - 263.84$$

$$NL(3, 4) = 1.008T_3 + 0.02116T_f(T_3 - T_4) + 2.065[\sec(\theta) - 1] - 273.69$$

$$NL(3, 4, 5) = 1.0006T_4 + 0.245(T_3 - T_5) + 0.02766T_f(T_3 - T_5) + 1.88[\sec(\theta) - 1] - 272.36$$

$$NL(4, 5) = 0.9604T_4 + 0.08752T_f(T_4 - T_5) + 0.852(T_4 - T_5)[\sec(\theta) - 1] - 261.46$$

Acknowledgments. The authors thank John Sapper and Charles Walton of NOAA/NESDIS for their assistance with the satellite-buoy matchup database and the various sea surface temperature algorithms. This work was sponsored by the Chief of Naval Operations (OP-096) under program element 63704N, Satellite Applications Program, with the Space and Naval Warfare Systems Command as program manager. NOARL contribution JA 321:067:92. This document is approved for public release; distribution is unlimited.

REFERENCES

Anding, D., and R. Kauth, Estimation of sea surface temperature from space, *Remote Sens. Environ.*, *1*, 217–220, 1970.

Barton, I., and R. Cechet, Comparison and optimization of AVHRR sea surface temperature algorithms, *J. Atmos. Oceanic Technol.*, *6*, 1083–1089, 1989.

Barton, I., A. Zavody, D. O'Brien, D. Cutten, R. Saunders, and D. Llewellyn-Jones, Theoretical algorithms for satellite-derived sea surface temperatures, *J. Geophys. Res.*, *94*, 3365–3375, 1989.

Bernstein, R., Sea surface temperature estimation using the NOAA

6 satellite Advanced Very High Resolution Radiometer, *J. Geophys. Res.*, *87*, 9455–9465, 1982.

Coppin, P. A., E. F. Bradley, I. J. Barton, and J. S. Godfrey, Simultaneous observations of sea surface temperature in the western equatorial Pacific Ocean by bulk, radiative, and satellite methods, *J. Geophys. Res.*, *96*, 3401–3409, 1991.

Eyre, J. R., On systematic errors in satellite sounding products and their climatological mean values, *Q. J. R. Meteorol. Soc.*, *113*, 279–292, 1987.

Hepplewhite, C. L., Remote observations of the sea surface and atmosphere: The oceanic skin effect, *Int. J. Remote Sens.*, *10*, 801–810, 1989.

Isemer, H., and L. Hasse, *The Bunker Climate Atlas of the North Atlantic Ocean*, Springer-Verlag, New York, 1985.

Kneizys, F. X., E. P. Shettle, L. W. Abreu, J. H. Chetwynd, G. P. Anderson, W. O. Gallery, J. E. A. Selby, and S. A. Clough, Users guide to LOWTRAN 7, *Rep. AFGL-TR-88-0177*, 137 pp., Air Force Geophys. Lab., Hanscom Air Force Base, Mass., 1988.

LaViolette, P. E., Processing satellite infrared and visible imagery for oceanographic analyses, in *Digital Image Processing in Remote Sensing*, edited by J. P. Muller, pp. 213–234, Taylor and Francis, Philadelphia, Pa., 1988.

Llewellyn-Jones, D., P. Minnett, R. Saunders, and A. Zavody, Satellite multi-channel infrared measurements of sea surface temperature of the N.E. Atlantic Ocean using AVHRR/2, *Q. J. R. Meteorol. Soc.*, *110*, 613–631, 1984.

Maul, G., and M. Sidran, Comment on "Estimation of sea surface temperature from space" by D. Anding and R. Kauth, *Remote Sens. Environ.*, *3*, 165–169, 1972.

McClain, E. P., Global sea surface temperatures and cloud clearing for aerosol optical depth estimates, *Int. J. Remote Sens.*, *10*, 763–769, 1989.

McClain, E. P., W. G. Pichel, and C. C. Walton, Comparative performance of AVHRR-based multichannel sea surface temperatures, *J. Geophys. Res.*, *90*, 11,587–11,601, 1985.

McMillin, L., Estimation of sea surface temperatures from two infrared window measurements with different absorption, *J. Geophys. Res.*, *80*, 5113–5117, 1975.

McMillin, L. M., and D. S. Crosby, Theory and validation of the multiple window sea surface temperature technique, *J. Geophys. Res.*, *89*, 3655–3661, 1984.

Minnett, P., A numerical study of the effects of anomalous North Atlantic atmospheric conditions on the infrared measurement of sea surface temperature from space, *J. Geophys. Res.*, *91*, 8509–8521, 1986.

Minnett, P., The regional optimization of infrared measurements of sea surface temperature from space, *J. Geophys. Res.*, *95*, 13,497–13,510, 1990.

Minnett, P., Consequences of sea surface temperature variability on the validation and applications of satellite measurements, *J. Geophys. Res.*, *96*, 18,475–18,489, 1991.

Prabhakara, C., G. Dalu, V. G. Kunde, Estimation of sea surface temperature from remote sensing in the 11- to 13-micrometer window region, *J. Geophys. Res.*, *79*, 5039–5044, 1974.

Robinson, I. S., N. C. Wells, and H. Charnock, The sea surface thermal boundary layer and its relevance to the measurement of sea surface temperature by air-borne and space-borne radiometers, *Int. J. Remote Sens.*, *5*, 19–45, 1984.

Schluessel, P., H.-Y. Shin, W. J. Emery, and H. Grassl, Comparison of satellite-derived sea surface temperatures with in situ skin measurements, *J. Geophys. Res.*, *92*, 2859–2874, 1987.

Strong, A. E., and E. P. McClain, Improved ocean surface temperatures from space—Comparison with drifting buoys, *Bull. Am. Meteorol. Soc.*, *65*, 138–142, 1984.

U.S. Air Force, Handbook of geophysics and space environments, report, Cambridge Res. Lab., Bedford, Mass., 1965.

Walton, C. C., Nonlinear multichannel algorithms for estimating sea surface temperature with AVHRR satellite data, *J. Appl. Meteorol.*, *27*, 115–124, 1988.

Walton, C. C., E. P. McClain, and J. F. Sapper, Recent changes in satellite-based multi-channel sea surface temperature algorithms, paper presented at Science and Technology for a New Oceans Decade, Mar. Technol. Soc., Washington, D. C., Sept. 1990.

R. J. Holyer and D. A. May, Department of the Navy, Naval Research Laboratory, Remote Sensing Applications Branch, Stennis Space Center, MS 39529-5004.

(Received October 23, 1992;
revised April 6, 1993;
accepted April 6, 1993.)